



Tetrapyrazinoporphyrazines with different number of peripheral pyridyl rings: Synthesis, photophysical and photochemical properties

Petr Zimcik*, Miroslav Miletin, Veronika Novakova, Kamil Kopecky, Zuzana Dvorakova

Department of Pharmaceutical Chemistry and Drug Control, Faculty of Pharmacy, Charles University, Heyrovského 1203, Hradec Kralove 50005, Czech Republic

ARTICLE INFO

Article history:

Received 10 June 2008

Received in revised form 17 July 2008

Accepted 19 July 2008

Available online 31 August 2008

Keywords:

Singlet oxygen

Fluorescence

Phthalocyanine

Tetrapyrazinoporphyrazine

Pyridyl

ABSTRACT

Zinc tetrapyrazinoporphyrazines comprising different numbers of pyridin-2-yl and *tert*-butylsulfanyl substituents were prepared by the statistical condensation of two precursors – 5,6-bis(*tert*-butylsulfanyl)pyrazine-2,3-dicarbonitrile (A) and 5,6-dipyridin-2-yl-pyrazine-2,3-dicarbonitrile (B). The ensuing zinc tetrapyrazinoporphyrazines were chromatographically separated on silica column and characterized. Adjacent (AABB) and opposite (ABAB) isomers were not separated. The prepared zinc tetrapyrazinoporphyrazines did not differ in their Q-band position but the B-band position was shifted hypsochromically for compounds bearing more pyridyl units; in addition, a weak band at 450–520 nm decreased with increasing number of pyridyl substituents. Singlet oxygen quantum yields (Φ_{Δ} in the range 0.69–0.53) decreased with increasing number of pyridyl units on the macrocyclic core, while fluorescence quantum yields showed the reverse tendency (Φ_F in the range 0.22–0.26).

© 2008 Elsevier Ltd. All rights reserved.

1. Introduction

Phthalocyanine (Pc) dyes have attracted much attention over a number of years [1]. Aza analogues of Pc, namely azaphthalocyanines (AzaPc), can be used in similar applications as their parent macrocycles [2]. Recently, we have investigated several tetrapyrazinoporphyrazines, a type of AzaPc, for their possible use in photodynamic therapy (PDT) [3–5]. This kind of medical treatment is based on production of cytotoxic species after illumination of a photosensitizer (e.g. porphyrins, chlorins, Pc) [6–8]. Photosensitizer absorbs the light and efficiently transfers the energy to ground state triplet oxygen forming highly reactive singlet oxygen that destroys the target tissues.

Peripheral pyridyls have been already used as substituents on Pc or AzaPc in relation to different applications. Tetrapyrazinoporphyrazines (TPyzPA) with eight pyridyl moieties have been investigated for their remarkable electron-deficient properties in electrochemistry both free and quarternized which allowed water solubility [9–12]. The same compounds have also been investigated for their non-linear optical properties [13]. Pyridyl moieties are also excellent substrates for metal-binding and can be used as ligands attached to Pc core [14]. Pyridyls bound to Pc

macrocycle through oxygen bridge have been tested as substituents also in photodynamic application [15–17].

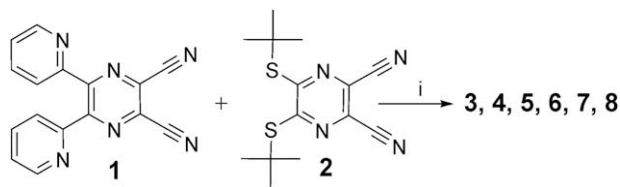
As it has been shown previously, peripheral substituents influence substantially the properties of AzaPc macrocycle. They may increase or, on the other hand, significantly decrease the production of singlet oxygen which is important for photodynamic action of AzaPc [18]. For example, alkylsulfanyl substituents were shown to belong among the most suitable for compounds in PDT. In presented work, we synthesized and studied photochemical and photophysical properties of TPyzPA derivatives bearing different number of pyridyl and *tert*-butylsulfanyl substituents. *Tert*-butylsulfanyls, in addition to the best influence on photodynamic properties, have also very good aggregation-inhibiting properties [19]. Aggregation is a common undesirable property of planar Pc, AzaPc and other porphyrinoid macrocycles and causes decrease of singlet oxygen and fluorescence quantum yields because the dynamics of excited aggregates become faster due to new non-radiative energy relaxation channels [20].

2. Experimental

All organic solvents used for the synthesis were of analytical grade. Anhydrous dimethylformamide (DMF) was purchased from Acros, 1,3-diphenylisobenzofuran (DPBF) from Aldrich. Zinc phthalocyanine (ZnPc) was obtained from Eastman Organic Chemicals (New York, USA). All chemicals were used as received except for zinc acetate dihydrate (Lachema, Czech Republic)

* Corresponding author. Tel.: +420 49 5067257; fax: +420 49 5067167.

E-mail address: petr.zimcik@faf.cuni.cz (P. Zimcik).



Scheme 1. Statistical condensation of compounds **1** and **2**. Reaction conditions: (i) anhydr. DMF, zinc acetate, 160 °C, 2 h.

which was dried at 78 °C under reduced pressure (13 mbar) for 5 h. TLC was performed on Merck aluminium sheets with silica gel 60 F₂₅₄. Merck Kieselgel 60 (0.040–0.063 mm) was used for column chromatography. Melting points were measured on Electrothermal IA9200 Series Digital Melting point Apparatus (Electrothermal Engineering Ltd., Southend-on-Sea, Essex, Great Britain) and are uncorrected. Infrared spectra were measured in KBr pellets on IR-Spectrometer Nicolet Impact 400. ¹H and ¹³C NMR spectra were recorded on Varian Mercury-Vx BB 300 (299.95 MHz – ¹H and 75.43 MHz – ¹³C). Chemical shifts reported are given relative to Si(CH₃)₄. UV–vis spectra were recorded on spectrophotometer UV-2401PC, Shimadzu Europa GmbH (Duisburg, Germany). MALDI-TOF mass spectra were recorded in positive reflectron mode on a mass spectrometer Voyager-DE STR (Applied Biosystems, Framingham, MA, USA). For each sample, 0.5 µl of the mixture was spotted onto the target plate, air-dried and covered with 0.5 µl of matrix solution consisting of 10 mg of α-cyano-4-hydroxycinnamic acid in 100 µl of 50% ACN in 0.1% trifluoroacetic acid. The instrument was calibrated externally with a five-point calibration using Peptide Calibration Mix1 (LaserBio Labs, Sophia-Antipolis, France).

Compound **2** was prepared according to previously published method [19]. Compound **1** was prepared according to literature [21]

with the small modification in eluent used for column chromatography purification (chloroform:acetone, 15:1 instead of published acetone).

2.1. Statistical condensation of compounds **1** and **2**

A mixture of **1** (569 mg, 2 mmol), **2** (613 mg, 2 mol) and anhydrous zinc acetate (2.56 g, 14 mmol) in anhydrous DMF was stirred on preheated oil bath at 160 °C for 2 h. The mixture was poured into distilled water and green precipitate was separated by filtration, washed with water and methanol and air-dried. The crude mixture was separated by column chromatography on silica using step gradient starting from chloroform:THF:pyridine, 100:6:1.5. The first eluted compound was symmetrical **3**. This compound showed the same characteristics as the standard already prepared in our laboratory by simple tetramerization of **2** [19]. The second green fraction contained compound **4** that was eluted using increased polarity of the mobile phase (chloroform:pyridine, 16:1). Further increase of eluent polarity to chloroform:pyridine, 6:1 led to isolation of isomers **5** and **6** as one fraction followed by compound **7**. Symmetrical **8** was not isolated from the column but prepared in a separate reaction according to published procedure [22]. Each fraction containing unsymmetrical TPzPA was further purified as mentioned below.

2.2. [2,3,9,10,16,17-Hexakis(tert-butylsulfanyl)-23,24-bis(pyridin-2-yl)-1,4,8,11,15,18,22,25-(octaaza)phtalocyaninato] zinc (II) (**4**)

The fraction with this compound was purified by preparative TLC on silica using toluene:pyridine, 7:1 as eluent (*R_f* 0.23). The spot was scrapped from the plate and product was extracted with pyridine, filtered and evaporated. The compound was isolated in minimal amount. MS (MALDI-TOF) *m/z* 1267 [M + H]⁺; 1211 [M-56 + H]⁺. UV–vis (pyridine) λ (nm) 657; 596; 385.

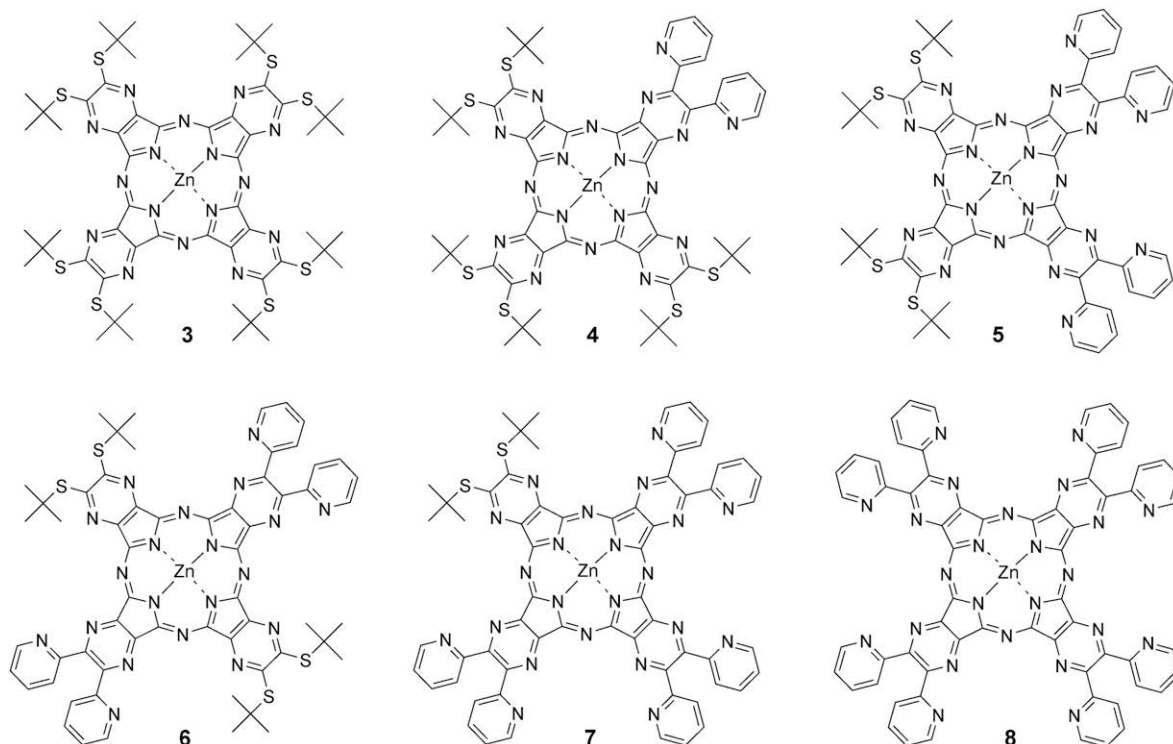


Fig. 1. Products of statistical condensation: compounds **3–8**.

Table 1
Photophysical, photochemical and spectral data of compounds **3–8** in pyridine

Compound	Absorbance (Q- and B-bands) λ_{\max} (nm)	Fluorescence λ_{\max} (nm)	Φ_F^b	Φ_A^b
3	657, 385	663	0.224	0.660
4	657, 384	665	0.226	0.688
5, 6	658, 383	665	0.229	0.586
7	657, 379	665	0.247	0.625
8^a	657, 374	665	0.257	0.531

^a Data for **8** corresponding to those published for this dye in Ref. [22].

^b A mean of three independent measurements. Estimated error $\pm 10\%$.

2.3. [2,3,16,17-Tetrakis(tert-butylsulfanyl)-9,10,23,24-terakis(pyridin-2-yl)-1,4,8,11,15,18,22,25-(octaaza)phtalocyaninato] zinc (II) (**6**) and [2,3,9,10-tetrakis(tert-butylsulfanyl)-16,17,23,24-terakis(pyridin-2-yl)-1,4,8,11,15,18,22,25-(octaaza)phtalocyaninato] zinc (II) (**5**)

These two isomers were isolated as one fraction with no detectable possibility of separation. The fraction was further purified on silica column using chloroform:pyridine, 6:1 as eluent. Pure fractions were evaporated and washed with methanol. Yield: 5 mg (0.4%) of dark green solid. MALDI-TOF m/z 1245 $[M + H]^+$; 1189 $[M - 56 + H]^+$. UV-vis (pyridine) λ (nm) 658; 596; 383. IR (KBr) ν (cm^{-1}) 3065; 2965; 2922; 2864; 1508; 1361; 1252; 1142; 1106; 1049; 980; 961. ^{13}C NMR ($\text{C}_6\text{D}_5\text{N}$) δ (ppm) 30.72; 30.79; 51.24; 51.34; aromatic signals not detected. ^1H NMR ($\text{C}_6\text{D}_5\text{N}$) δ (ppm) 8.94 (d; 2H; $J = 7$ Hz; pyridyl H-3); 8.67–8.62 (m; 2H; pyridyl H-3); 8.58 (d; 4H; $J = 5$ Hz; pyridyl H-6); 8.15 (td; 4H; $J_1 = 8$ Hz; $J_2 = 1$ Hz; pyridyl H-4); 7.38 (dd; 2H; $J_1 = 7$ Hz; $J_2 = 5$ Hz; pyridyl H-5); 7.30–7.21 (m; 2H; pyridyl H-5); 2.27 (s; 18H; CH_3); 2.03 (s; 18H; CH_3).

2.4. [2,3-Bis(tert-butylsulfanyl)-9,10,16,17,23,24-hexakis(pyridin-2-yl)-1,4,8,11,15,18,22,25-(octaaza)phtalocyaninato] zinc (II) (**7**)

The fraction was further purified on silica column using chloroform:pyridine, 6:1 as eluent. Pure fractions were evaporated and

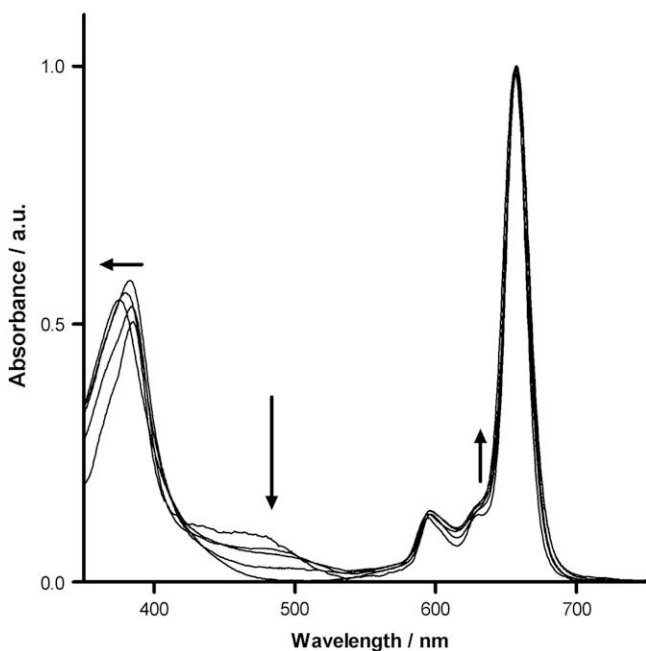


Fig. 2. UV-vis absorption spectra of compounds **3–8** in pyridine. Spectra were normalized to the same absorption in the Q-band. Arrows indicate differences arising in the spectra due to increasing number of pyridyl substituents.

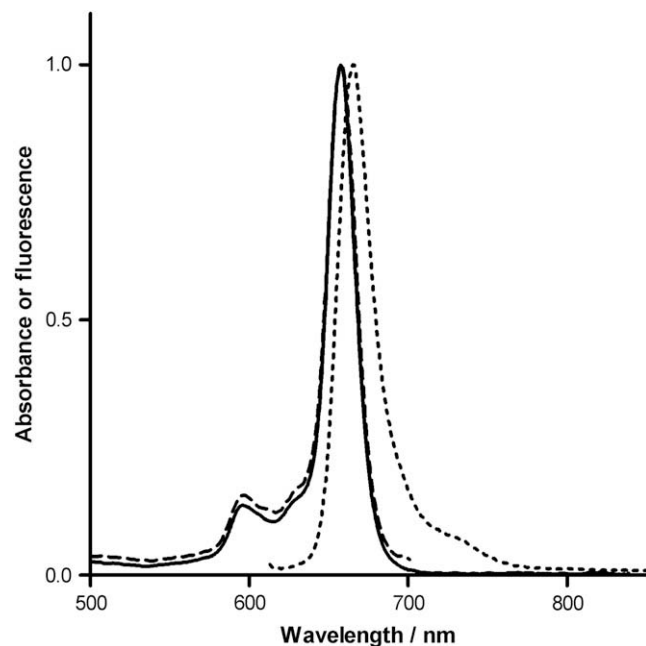


Fig. 3. Normalized absorption (full line), fluorescence emission (dotted), fluorescence excitation (dashed) spectra of **7** in pyridine.

washed with methanol. Yield: 8 mg (0.6%) of dark green solid. MALDI-TOF m/z 1223 $[M + H]^+$; 1167 $[M - 56 + H]^+$. UV-vis (pyridine) λ (nm) 657; 595; 378. ^{13}C NMR ($\text{C}_6\text{D}_5\text{N}$) δ (ppm) 30.72; 51.19; 125.30; 125.46; 125.58; 136.70; 136.76; 137.17; 145.75; 148.89; 149.11; 151.70; 151.72; 151.99; 152.79; 153.63; 154.52; 154.58; 154.62; 158.53; 159.20; 159.58. ^1H NMR ($\text{C}_6\text{D}_5\text{N}$) δ (ppm) 8.97 (d; 2H; $J = 8$ Hz; pyridyl H-3); 8.68–8.62 (m; 4H; pyridyl H-3); 8.59 (d; 2H; $J = 4$ Hz; pyridyl H-6); 8.35–8.21 (m; 4H; pyridyl H-6); 8.16 (td; 2H; $J_1 = 8$ Hz; $J_2 = 1$ Hz; pyridyl H-4); 7.73–7.61 (m; 4H; pyridyl H-4); 7.40 (ddd; 2H; $J_1 = 8$ Hz; $J_2 = 5$ Hz; $J_3 = 1$ Hz; pyridyl H-5); 7.33–7.23 (m; 4H; pyridyl H-5); 2.08 (s; 18H; CH_3).

2.5. Singlet oxygen measurements

Singlet oxygen production was monitored as DPBF decomposition reactions, as reported previously [23]. Stock solution (2.5 ml) of DPBF in pyridine (5×10^{-5} M) was transferred to a 10×10 mm quartz optical cell and bubbled with oxygen for 1 min; a pyridine stock solution of the dye ($\sim 30 \mu\text{l}$) was then

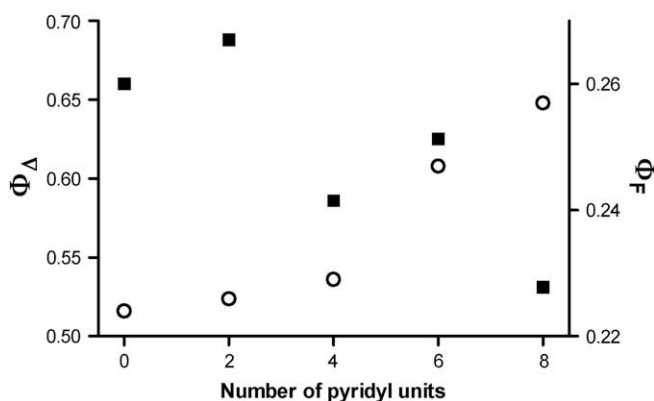


Fig. 4. Values of Φ_F (○) and Φ_A (■) TPzPA (**3–8**) in pyridine in dependence on the number of pyridyl units bound peripherally.

added (the absorbance of the dye solution at the Q-band maximum was always ~ 0.1). The solution was then stirred and irradiated for different times using a halogen lamp (Tip, 200 W), the incident light being filtered through a water filter (6 cm) and an orange HOYA G filter to remove infrared light and light < 506 nm, respectively. A decrease of a DPBF amount in solution (maximum 15%) was measured as the decrease in its absorbance at 415 nm. Calculations of singlet oxygen quantum yield were then performed according to published equations [23]. ZnPc in pyridine was used as the reference ($\Phi_{\Delta} = 0.61$) [24].

2.6. Fluorescence measurements

Fluorescence quantum yields of the dyes were determined in pyridine and calculated according to following equation (Eq. (1)):

$$\Phi_F^S = \Phi_F^R \frac{F^S}{F^R} \frac{1 - 10^{-A^R}}{1 - 10^{-A^S}} \quad (1)$$

where Φ_F is fluorescence quantum yield, F is integrated area under the emission spectrum and A is absorbance at excitation wavelength. Superscripts R and S correspond to reference and sample, respectively. ZnPc in pyridine was used as reference ($\Phi_F = 0.20$ in pyridine [24]). The dye solutions prepared as mentioned above were used for measurements after appropriate dilution. In all cases the absorbance at λ_{\max} of the Q-band was below 0.05 in order to minimize reabsorption of the emitted light. Fluorescence emission spectra were recorded after excitation at 606 nm. Fluorescence excitation spectra were recorded observing the fluorescence signal at 725 nm.

3. Results and discussion

3.1. Synthesis and characterization

The macrocycle of TPyzPA is usually formed by cyclo-tetramerization of suitably substituted pyrazine-2,3-dicarbonitriles [2]. If two different precursors (A and B) are used in one reaction, a statistical mixture of six different compounds of AAAA, AAAB, ABAB, AABB, ABBA and BBBB type will arise. Although several methods have been developed for selective synthesis of each unsymmetrical derivative [25], the above mentioned statistical condensation is the simplest and the most suitable when all derivatives in the mixture are of investigation interest. That is why, a statistical condensation of precursors **1** and **2** (Scheme 1) in anhydrous DMF in the presence of zinc acetate was chosen for synthesis of the mixture of six desired products **3–8** (Fig. 1). The products **3–7** were separated chromatographically on silica column. The fractions were assigned to the right structures on the basis of MS MALDI-TOF spectrometry and ^1H NMR spectroscopy. Compound **8** eluted as the last one was not isolated but for simplicity prepared in a separate reaction directly from precursor **1** according to previously published method [22]. The yields of compounds bearing more pyridyl moieties were significantly lowered by strong silica binding properties which did not allow full recovery of the compounds from column. Since each fraction had to be purified using column chromatography at least once more (usually twice), the final yields were only in the range 0.4–0.6%. The eluent contained some amount of pyridine in order to minimize losses; unfortunately even such approach did not bring the satisfactory results. The yield of compound **4** was almost negligible (as deduced also from intensity of the spots on TLC) perhaps due to reactivity reasons and this compound was isolated in minimal amount using preparative TLC. Such small amount allowed only confirmation of the right mass using MALDI-TOF mass spectrometry and subsequent tests on photophysical and photochemical

properties. Compounds bearing four pyridyl substituents can form two positional isomers – adjacent (**5**) and opposite (**6**). However, only one fraction with the mass corresponding to these compounds was isolated and ^1H NMR spectroscopy indicated a mixture of both isomers. Both isomers eluted on TLC with the same R_f values and we did not even observe any separation into two spots.

3.2. UV-vis and fluorescence spectra

All prepared compounds showed UV-vis spectrum typical for TPyzPA. As obvious from Table 1, position of Q-bands is not influenced by peripheral substitution (see also Fig. 2). It means that influence of both types of substituents on bathochromic shift of the Q-band may be considered equal. Compared to unsubstituted ZnTPyzPA (636 nm), the red-shift of 20 nm is important. Position of B-band shifts slightly hypsochromically with increasing number of pyridyl substituents. The band in area 450–520 nm that appears in the spectrum of compounds containing some *tert*-butylsulfanyls is attributed to $n-\pi^*$ transitions of the lone pair of the sulfur. As can be seen from Fig. 2, the intensity of the band in this area decreases along with decreasing number of *tert*-butylsulfanyl substituents and completely diminishes at compound **8** with only pyridyl substituents. Similar observations have been already described in the similar series of compounds with different number of alkyl-sulfanyl and butoxycarbonyl substituents [26]. The intensity of this band also influences the color of the dye's pyridine solution which gradually changes from grass green for **3** to cyan blue for **8**. A well resolved small maximum in the Q-band of **3** at 630 nm slightly loses its fine character and flattens (indicated by arrow in the Fig. 2). For compounds bearing more pyridyl substituents it becomes only a bad resolved shoulder.

It is a typical behavior of unsymmetrically substituted Pc and AzaPc that their Q-bands are split due to loss of the whole symmetry of the macrocycle [27–29]. However, this is not our case. All dyes **3–8** showed only single, non-split and non-degenerated Q-band. The explanation is the following: the difference in bathochromic shifts of the Q-band between the outer members of our series (**3** and **8**) is not observable (see Table 1) therefore influence of both pyridyl and *tert*-butylsulfanyl substituents on the spectral properties of the whole macrocycle in the Q-band area can be considered equal. As a consequence, regardless of which substituent will be placed on the periphery, the position of the Q-band will be always the same and no splitting will occur.

Fluorescence emission spectra of all compounds were similar and of typical character for TPyzPA (Fig. 3) with only small Stokes shift approximately 7 nm. A perfect correspondence of excitation spectrum and absorption spectrum (Fig. 3) confirms purity of the compounds and exclusively monomeric character of the dissolved dyes. The dimers or higher aggregates, which can be formed in solution, alter significantly the absorption spectrum but not the excitation spectrum. Presence of only monomers is also important prerequisite for proper measurements of the quantum yields which could be influenced by possible dimers formation. Since the pyridine solutions contained only monomers, the differences in measured values of quantum yields (Section 3.3) may be attributed solely to influences of peripheral substituents.

3.3. Singlet oxygen and fluorescence quantum yields

Singlet oxygen quantum yield has been determined using a DPBF decomposition method. Data received are presented in Table 1 and Fig. 4. Despite a mild variation in the Φ_{Δ} values, there is a general tendency of singlet oxygen quantum yields to decrease with increasing number of pyridyl units. However, even for the compound **8**, the singlet oxygen production is still high with

sufficient Φ_{Δ} values ensuring efficient photosensitization. Therefore all of the compounds may be potentially used in PDT application.

Similar dependence can be observed for fluorescence quantum yield. However, in this case the Φ_F values increases with the increasing number of pyridyls on macrocyclic core. Such observations are understandable since the fluorescence and intersystem crossing (responsible for triplet state formation and subsequently singlet oxygen production) are the competitive ways of relaxation of the excited singlet state of photosensitizers. On the basis of these results we suggest that *tert*-butylsulfanyl substituents in the presented compounds activate the TPyzPA macrocycle toward stronger singlet oxygen production while the pyridyls lead to slightly stronger production of fluorescence comparing to former substituents.

From our results, it seems that the influence of the peripheral substituents on Φ_F and Φ_{Δ} values can be considered as an additive property. These results are supported by our former investigations on the properties of TPyzPA with different number of butoxycarbonyl and *tert*-butylsulfanyl substituents [26] where we found very similar relations to those obtained in this work.

4. Conclusions

Using a statistical condensation, we prepared, isolated and characterized TPyzPA substituted with different number of *tert*-butylsulfanyl and pyridyl substituents. Unfortunately, due to strong silica binding properties, the yields of unsymmetrical compounds were very low. Investigations on their photophysical and photochemical properties together with former results lead us to conclusion that influence of peripheral substituents may be considered as the additive function. These observations may be employed in future to predict roughly the above discussed properties knowing only the outer members of compounds series. A fine tuning of the Φ_F and Φ_{Δ} values could be also possible.

Acknowledgements

The work was supported by Czech Science Foundation, grant No. 203/07/P445 and by the research project MSM0021620822.

References

- [1] Kadish KM, Smith KM, Guillard R. The porphyrin handbook. New York: Academic Press; 2003.
- [2] Stuzhin PA, Ercolani C. In: Kadish KM, Smith KM, Guillard R, editors. The porphyrin handbook, vol. 15. New York: Academic Press; 2003. p. 263–364.
- [3] Zimcik P, Miletin M, Musil Z, Kopecky K, Kubza L, Brault D. J Photochem Photobiol A Chem 2006;183:59–69.
- [4] Zimcik P, Miletin M, Musil Z, Kopecky K, Slajsova D. Dyes Pigment 2008;77:281–7.
- [5] Zimcik P, Mørkved EH, Andreassen T, Lenco J, Novakova V. Polyhedron 2008;27:1368–74.
- [6] Brown SB, Brown EA, Walker I. Lancet Oncol 2004;5:497–508.
- [7] Nyman ES, Hynninen PH. J Photochem Photobiol B Biol 2004;73:1–28.
- [8] Juzeniene A, Peng Q, Moan J. Photochem Photobiol Sci 2007;6:1234–45.
- [9] Bergami C, Donzello MP, Ercolani C, Monacelli F, Kadish KM, Rizzoli C. Inorg Chem 2005;44:9852–61.
- [10] Bergami C, Donzello MP, Monacelli F, Ercolani C, Kadish KM. Inorg Chem 2005;44:9862–73.
- [11] Donzello MP, Ou Z, Dini D, Meneghetti M, Ercolani C, Kadish KM. Inorg Chem 2004;43:8637–48.
- [12] Donzello MP, Ou Z, Monacelli F, Ricciardi G, Rizzoli C, Ercolani C, et al. Inorg Chem 2004;43:8626–36.
- [13] Villano M, Amendola V, Sandona G, Donzello MP, Ercolani C, Meneghetti M. J Phys Chem B 2006;110:24354–60.
- [14] Haas M, Liu SX, Neels A, Decurtins S. Eur J Org Chem 2006;5467–78.
- [15] Scalise N, Durantini EN. Bioorg Med Chem 2005;13:3037–45.
- [16] Mantareva V, Petrova D, Avramov L, Angelov I, Borisova E, Peeva M, et al. J Porphyr Phthalocyanines 2005;9:47–53.
- [17] Michelsen U, Kliesch H, Schnurpfeil G, Sobbi AK, Wöhrle D. Photochem Photobiol 1996;64:694–701.
- [18] Zimcik P, Miletin M, Kostka M, Schwarz J, Musil Z, Kopecky K. J Photochem Photobiol A Chem 2004;163:21–8.
- [19] Kostka M, Zimcik P, Miletin M, Klemra P, Kopecky K, Musil Z. J Photochem Photobiol A Chem 2006;178:16–25.
- [20] Lang K, Mosinger J, Wágnerová DM. Coord Chem Rev 2004;248:321–50.
- [21] Mørkved EH, Ossletten H, Kjøsen H. J Prakt Chem 2000;342:83–6.
- [22] Mørkved EH, Afseth NK, Zimcik P. J Porphyr Phthalocyanines 2007;11:130–8.
- [23] Musil Z, Zimcik P, Miletin M, Kopecky K, Link M, Petrik P, et al. J Porphyr Phthalocyanines 2006;10:122–31.
- [24] Ogunsipe A, Maree D, Nyokong T. J Mol Struct 2003;650:131–40.
- [25] De La Torre G, Claessens CG, Torres T. Eur J Org Chem 2000:2821–30.
- [26] Musil Z, Zimcik P, Miletin M, Kopecky K, Petrik P, Lenco J. J Photochem Photobiol A Chem 2007;186:316–22.
- [27] Musil Z, Zimcik P, Miletin M, Kopecky K, Lenco J. Eur J Org Chem 2007:4535–42.
- [28] Linszen TG, Hanack M. Chem Ber 1994;127:2051–7.
- [29] Sakamoto K, Kato T, Cook MJ. J Porphyr Phthalocyanines 2001;5:742–50.